# The E3 ubiquitin ligase LNX1p80 promotes the removal of claudins from tight junctions in MDCK cells

**Senye Takahashi[1,*,‡], Noriko Iwamoto[1,2,*], Hiroyuki Sasaki[3], Masato Ohashi[4], Yukako Oda[2], Shoichiro Tsukita[1,§] and Mikio Furuse[2,¶]**

[1]Department of Cell Biology, Graduate School of Medicine, Kyoto University, Yoshida-Konoe, Sakyo-ku, Kyoto 606-8501, Japan
[2]Division of Cell Biology, Department of Physiology and Cell Biology, Graduate School of Medicine, Kobe University, Kusunoki-cho 7-5-1, Chuo-ku, Kobe 650-0017, Japan
[3]Department of Molecular Cell Biology, Institute of DNA Medicine, The Jikei University School of Medicine, Nishi-Shinbashi, Minato-ku, Tokyo 105-8461, Japan
[4]Laboratory of Nano-Structure Physiology, Okazaki Institute for Integrative Bioscience, National Institutes of Natural Sciences, Higashiyama 5-1, Myodaiji-cho, Okazaki 444-8787, Japan

*These authors contributed equally to this work
‡Present address: Graduate School of Pharmaceutical Sciences, Kyoto University, Yoshida-shimoadachi, Sakyo-ku, Kyoto 606-8501, Japan
§Deceased December 2005
¶Author for correspondence (e-mail: furuse@med.kobe-u.ac.jp)

*Accepted 27 November 2008*
*Journal of Cell Science 122, 985-994 Published by The Company of Biologists 2009*
*doi:10.1242/jcs.040055*

## Summary

**The structural continuity of tight junctions (TJs) is consistently maintained even when epithelial cells divide and move within the cellular sheet. This process is associated with dynamic remodeling of TJs by coordinated internalization and generation of claudin-based TJ strands, but the molecular mechanism behind the regulated turnover of TJs remains largely unknown. In this study, we identified the p80 isoform of the E3 ubiquitin ligase ligand of Numb-protein X1 (LNX1p80) as a protein binding to claudin-1. Interestingly, the concentration of claudins in TJs was remarkably reduced when LNX1p80 was overexpressed in MDCK cells, and there was a reduction not only in the number of TJ strands but also in the amount of detergent-insoluble claudins. We also found that LNX1p80 promoted polyubiquitylation of claudins. This ubiquitylation is dependent on its RING-finger domain and is not mediated by Lys48 of ubiquitin, which is used for protein degradation by the proteasome. Furthermore, LNX1p80 was often colocalized with claudins in vesicular structures containing markers for late endosomes and lysosomes. These findings suggest that LNX1p80 is involved in the ubiquitylation, endocytosis and lysosomal degradation of claudins, and that the turnover of TJs is regulated by ubiquitylation.**

Key words: Tight junctions, Claudin, Ubiquitylation, LNX1, E3 ubiquitin ligase

## Introduction

The epithelium and endothelium separate many distinct fluid compartments in the body of metazoans, which is fundamental to the physiological functions of most organ systems. When epithelial and endothelial cellular sheets work as barriers for this compartmentalization, the intercellular space must be sealed to avoid leakage of solutes (Powell, 1981). Tight junctions (TJs) have a crucial role in this epithelial and endothelial barrier function by restricting the diffusion of solutes through the paracellular pathway (Van Itallie and Anderson, 2006; Furuse and Tsukita, 2006; Angelow et al., 2008). More precisely, TJs are not complete barriers, but regulate the passive flow of small molecules in a size- and charge-selective manner. The barrier property of TJs varies among cell types depending on their physiological functions.

Several types of integral membrane proteins have been shown to be localized at TJs, such as occludin, claudins, tricellulin and immunoglobulin-like membrane proteins including the junction adhesion molecule (JAM) family, coxsackievirus and adenovirus receptor (CAR), endothelial cell-selective adhesion molecule (ESAM) etc. (Chiba et al., 2008). Among them, claudins are a major constituent of intramembranous structures of TJs (TJ strands) and are directly involved in intercellular sealing. Claudins, which have molecular masses of ~23 kDa, have four transmembrane domains and two extracellular loops, and are comprised of a multi-gene family consisting of ~24 members (Furuse et al., 1998a; Van Itallie and Anderson, 2006; Furuse and Tsukita, 2006; Angelow et al., 2008). When claudins are overexpressed in mouse L fibroblasts, exogenous claudins reconstitute TJ strands de novo by polymerizing within plasma membranes and associate between adjacent cells (Furuse et al., 1998b). In most epithelial cells, multiple claudin types are coexpressed in individual cells, where TJ strands are thought to be a mosaic of these claudins (Furuse et al., 1999). Each cell type expresses a unique set of claudins in various combinations and ratios and each claudin has a unique potential role in the barrier property of TJs, such as conductance and charge selectivity (Van Itallie and Anderson, 2006; Furuse and Tsukita, 2006; Angelow et al., 2008). Thus, the variation in the expression pattern of claudins creates a functional diversity of TJs depending on the physiological requirement of each cell type. Furthermore, recent analyses of phenotypes in claudin gene knockout mice and human hereditary diseases with mutations in claudin family genes have revealed a crucial role of TJs in various organ systems in vivo (Furuse and Tsukita, 2006).

Although the barrier function of the cellular sheet must be stably maintained, TJs are thought to be dynamically rearranged when individual cells move against adjacent cells (Matsuda et al., 2004). Upon cell division, for example, the structural continuity of TJs is maintained in spite of a remarkable change in cell shape (Jinguji

and Ishikawa, 1992; Baker and Garrod, 1993). Striking rearrangements of cells within epithelial cellular sheets are also observed during morphogenetic processes during development. For example, in convergent extension and germ band extension, cells exhibit 'intercalation', in which a cell slides against adjacent cells and the whole shape of the cellular sheet elongates (Gumbiner, 1996; Schock and Perrimon, 2002). In these conditions, TJs are believed to be repeatedly remodeled to fulfil two apparently contradictory roles: the rearrangement of cells within cellular sheets and the maintenance of the epithelial barrier function as a whole. There must be a coordinated regulatory mechanism to reconcile these phenomena, but its molecular mechanisms are mostly unknown. In our previous study, we succeeded in visualizing the endocytosis of GFP-tagged claudin-3 from TJs in epithelial cells by time-lapse fluorescence microscopy (Matsuda et al., 2004). This endocytosis of claudins was frequently observed when TJs between two adjacent cells decreased in length as cell-cell junctions were remodeled. The manner of claudin internalization was peculiar; tightly apposed TJ membranes were endocytosed without being detached into one of the adjoining cells. Interestingly, internalized claudin-containing vesicles do not include the integral membrane protein occludin or the claudin-binding plaque protein ZO-1, suggesting that claudins are selectively segregated and endocytosed from TJs (Matsuda et al., 2004). To date, however, the molecular mechanism behind this internalization has not been clarified.

One of the possible mechanisms underlying the selective internalization of integral membrane proteins is their modification with ubiquitin (ubiquitylation), followed by their recognition by ubiquitin-binding proteins that are involved in endocytic vesicle budding (Hicke and Dunn, 2003; d'Azzo et al., 2005; Mukhopadhyay and Riezman, 2007). Ubiquitin is a 76 amino acid protein that forms a stable conjugation with other proteins by the action of three enzymes: a ubiquitin-activating enzyme (E1), a ubiquitin-conjugating enzyme (E2) and a ubiquitin ligase (E3) (Hershko and Ciechanover, 1998). In addition to the 26S proteasome-mediated protein degradation, ubiquitylation is often used as a signal for various cellular processes, including endocytosis and trafficking for lysosomal degradation (Hicke and Dunn, 2003; d'Azzo et al., 2005; Mukhopadhyay and Riezman, 2007). To date, a number of integral membrane proteins, such as G-protein-coupled receptors, receptor tyrosine kinases, membrane transporters and immune molecules, have been reported to be regulated by ubiquitin-dependent sorting (Hicke and Dunn, 2003). Among cell-adhesion-related proteins, E-cadherin, a key adhesion molecule of adherens junctions, is ubiquitylated by the RING-type E3 ubiquitin ligase Hakai (Fujita et al., 2002). Expression of Hakai in cultured epithelial cells enhances endocytosis of E-cadherin, leading to the disruption of cell-cell contacts and promotion of cell motility. Occludin, a TJ-associated integral membrane protein, interacts with the HECT-type E3 ubiquitin ligase Itch and is ubiquitylated (Traweger et al., 2002). However, there have been no reports on the ubiquitylation of claudins, which are key membrane components for the structure and the barrier function of TJs.

In this study, we identified LNX1p80, an E3 ubiquitin ligase, as a binding partner of claudin-1 by yeast two-hybrid screening. Interestingly, the overexpression of LNX1p80 in MDCK cells remarkably reduced the concentration of claudins in TJ regions. We also found that LNX1p80 promoted the ubiquitylation of claudin-1 and colocalized with claudins in endocytic vesicular structures. These findings suggest that LNX1p80 is involved in the dynamic remodeling of TJs by selective ubiquitylation, endocytosis, and degradation of claudins.

## Results

### LNX1 is a claudin-1-binding protein

To identify novel claudin-binding proteins involved in the regulation of TJ formation, we performed yeast two-hybrid screening using a mouse brain cDNA library with the C-terminal cytoplasmic region of claudin-1 as bait. Among positive clones, four contained identical cDNA fragments encoding residues 1-146 of ZO-1, including its PDZ1 domain. This result was expected because the C-terminal cytoplasmic domain of claudin is known to bind to the PDZ1 domain of ZO-1 (Itoh et al., 1999). The other three clones encoded residues 256-729 of mouse ligand of Numb-protein X1 (LNX1), including four PDZ domains. LNX1 was originally identified as a binding partner of Numb by yeast two-hybrid screening and was also reported to be involved in ubiquitylation and degradation of Numb (Dho et al., 1998; Nie et al., 2002). LNX1 has two splicing variants, p70 and p80. LNX1p70 consists of the N-terminal Numb binding region and four PDZ domains, whereas LNX1p80 has an additional RING-finger domain at the N-terminus followed by a Numb-binding region and four PDZ domains (Fig. 1A). Because the RING-finger domain has not been reported as a domain component of TJ-associated proteins, we selected LNX1p80 for further analyses. We cloned the full-length mouse LNX1p80 (mLNX1p80) cDNA and confirmed the interaction of LNX1p80 protein with the C-terminus of claudin-1 in in vitro binding assays. The GST-fusion proteins with the C-terminal cytoplasmic domain of claudin-1, RKTTSYPTPRPYPKPTPSSGKDYV, and its mutant lacking C-terminal tyrosine and valine (YV-deleted mutant) were bound to glutathione-conjugated beads and incubated with the lysate of HEK293 cells expressing HA-tagged mLNX1p80. The bound proteins were eluted with these GST-fusion proteins and separated by SDS-PAGE, followed by immunoblotting with anti-HA monoclonal antibody. As shown in Fig. 1B, HA-tagged mLNX1p80 associated with the C-terminal cytoplasmic domain of claudin-1 but not with its YV-deleted mutant.

### LNX1p80 downregulates claudins from TJs in MDCK cells

To examine subcellular localization of LNX1p80 in epithelial cells, we overexpressed EGFP-tagged mLNX1p80 (EGFP-mLNX1p80) in MDCK cells and their GFP signals were compared with immunofluorescently labeled ZO-1. Exogenous EGFP-mLNX1p80 exhibited a linear localization circumscribing cells in addition to cytoplasmic distribution (Fig. 2A). This linear localization of EGFP-mLNX1p80 colocalized with ZO-1, suggesting that at least part of EGFP-mLNX1p80 localized to the apical junctional complex, including TJs. Furthermore, very interestingly, we found that claudin-1 concentrations at TJs were remarkably reduced in MDCK cells overexpressing EGFP-mLNX1p80. This effect could be clearly visualized when these cells were co-cultured with parent MDCK cells, followed by immunofluorescent staining with anti-claudin-1 polyclonal antibody (Fig. 2B).

To confirm the reduction of claudin-1 in TJs upon overexpression of LNX1p80, we then generated MDCK cell lines with a stable expression of N-terminal EGFP-tagged canine LNX1p80 (EGFP-LNX1p80) under the control of the Tet-Off system. In these cells, expression of EGFP-LNX1p80 was induced by removing doxycycline from the medium (Dox–) and was suppressed by adding doxycycline to the medium (Dox+). EGFP-LNX1p80 was undetectable on western blots when doxycycline was present, but

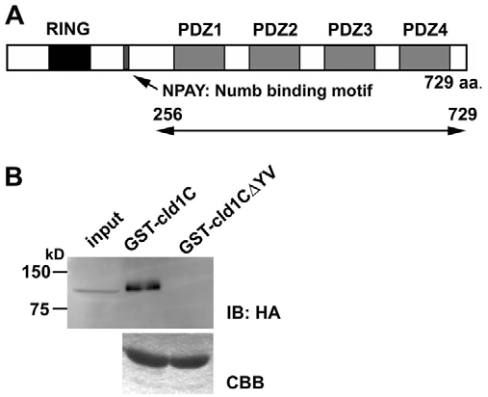


**Fig. 1.** Identification of LNX1p80 as a claudin-1-binding protein. (A) Schematic representation of LNX1p80. LNX1p80 contains a RING-finger domain, followed by a NPAY motif for interaction with Numb, and four PDZ domains. A cDNA fragment encoding residues 256-729 of mouse LNX1p80 (mLNX1p80), which includes four PDZ domains, was obtained in yeast two-hybrid screening with the C-terminal cytoplasmic domain of claudin-1 as bait. (B) Interaction of mLNX1p80 with the cytoplasmic domain of claudin-1 in vitro. HA-tagged mLNX1p80 bound to the GST-fusion proteins with the C-terminal cytoplasmic domain of claudin-1 (GST-cld1C) or its mutant lacking C-terminal tyrosine and valine (GST-cld1CΔYV) was detected in western blots with anti-HA mAb (IB: HA). The amount of eluted GST-fusion proteins is shown by Coomassie brilliant blue staining (CBB).

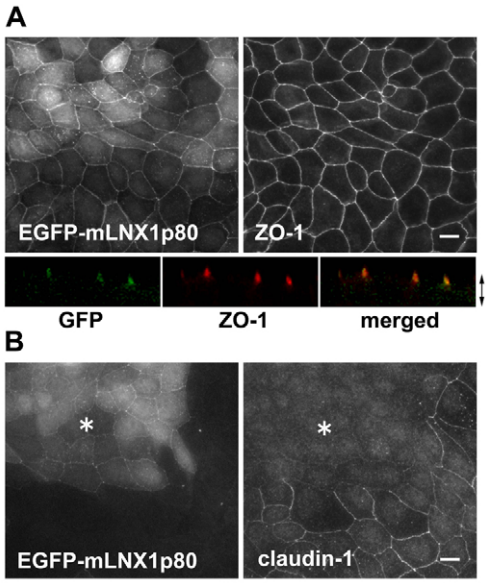


**Fig. 2.** Localization of exogenous LNX1p80 in MDCK cells. (A) MDCK cells stably expressing EGFP-tagged mouse LNX1p80 (EGFP-mLNX1p80) were immunofluorescently stained with anti-ZO-1 mAb. The localization of EGFP-mLNX1p80 in the same field was detected with its fluorescent signal. EGFP-mLNX1p80 colocalized with ZO-1 at cell-cell junctions and was also distributed in the cytoplasm. Vertical sectional images obtained from confocal microscopy showed that EGFP-mLNX1p80 was colocalized with ZO-1 at the most apical portion of lateral membranes. Arrow indicates the thickness of the cellular sheet. (B) EGFP-mLNX1p80-expressing MDCK cells were co-cultured with parental MDCK cells and immunostained with anti-claudin-1 pAb. The concentration of claudin-1 in TJs was remarkably reduced in EGFP-mLNX1p80-expressing cells (asterisk). Scale bars: 10 μm.

was expressed when doxycycline was removed (Fig. 3A). By immunofluorescent staining, we confirmed that the expression of EGFP-LNX1p80 was induced upon doxycycline removal, although some cells did not appear to respond to the removal of doxycycline. The concentration of claudin-1 in TJs was remarkably reduced in EGFP-LNX1p80-induced MDCK cells (Fig. 3B). Normal concentrations of claudin-1 at TJs were detected only in cells where EGFP-LNX1p80 expression was not induced. Junctional concentrations of claudin-2 and claudin-4 were remarkably reduced, similarly to claudin-1 in EGFP-LNX1p80-induced MDCK cells, whereas occludin staining was moderately decreased (Fig. 3C). By contrast, the localization of ZO-1, a claudin-binding plaque protein, and E-cadherin, an adherens junction (AJ)-associated adhesion molecule, did not change significantly (Fig. 3C).

We then attempted to analyze the ultrastructure of TJs in EGFP-LNX1p80-expressing MDCK cells. However, as a significant cell population did not express EGFP-LNX1p80 in our Tet-Off MDCK system, this hampered electron microscopic as well as biochemical analyses. To overcome this problem, we obtained MDCK cells, almost all of which expressed EGFP-LNX1p80, by introducing its cDNA into MDCK cells via a retrovirus vector, followed by collection of GFP signal-positive cells by fluorescence-activated cell sorting. We also generated EGFP-expressing MDCK cells as controls by using the same protocol. We propagated each cell population and confirmed that the concentration of claudins in cell-cell junctions was markedly reduced in EGFP-LNX1p80-expressing cells compared with EGFP-expressing cells as observed by immunofluorescence staining (Fig. 4A). The morphology of TJs in these two cell populations was then examined by freeze-fracture replica electron microscopy. As shown in Fig. 4B, the network of TJ strands in EGFP-LNX1p80-expressing cells was much less developed than that in EGFP-expressing control cells. Next, we analyzed the barrier properties of TJs in these cells. When EGFP-expressing control cells were trypsinized and cultured on permeable filters for 6 days, the transepithelial electric resistance (TER) initially reached to ~200 Ω $cm^2$ and then settled down to ~60 Ω $cm^2$. Under the same culture conditions, the TER of EGFP-LNX1p80-expressing MDCK cells gradually increased to ~60 Ω $cm^2$ (Fig. 5A), although the cells never exhibited any growth defects (data not shown). The paracellular flux of 4 kDa FITC-dextran across confluent EGFP-LNX1p80-expressing MDCK cells was about tenfold larger than that across EGFP-expressing control cells (Fig. 5B). These results suggest that LNX1p80 expression remarkably affects the TJ barrier properties.

### LNX1p80 promotes ubiquitylation of claudins

LNX1p80 binds to claudin-1 and contains a RING-finger domain, which is a hallmark of RING-type E3 ubiquitin ligases. Thus, we examined whether LNX1p80 has claudin ubiquitylation activity. For this purpose, we coexpressed canine claudin-1, HA-tagged ubiquitin and Flag-tagged canine LNX1p80 (FLAG-LNX1p80) in HEK293 cells. After 36 hours of transfection, claudin-1 was immunoprecipitated from the cell lysate followed by detection of ubiquitylation by immunoblotting with anti-HA antibody. The smear pattern of HA signal in the precipitates with Flag-LNX1p80 on the blotted membrane was significantly stronger than that with a control vector, indicating that Flag-LNX1p80 promotes ubiquitylation of claudin-1 (Fig. 6A). Ubiquitylation of claudin-2 and claudin-4 was detected in the same experiments (data not shown). When the RING-finger domain mutant of Flag-LNX1p80, in which a conserved Cys48 in a RING-finger domain was substituted with alanine (Flag-LNX1p80C48A) (Nie et al., 2002),

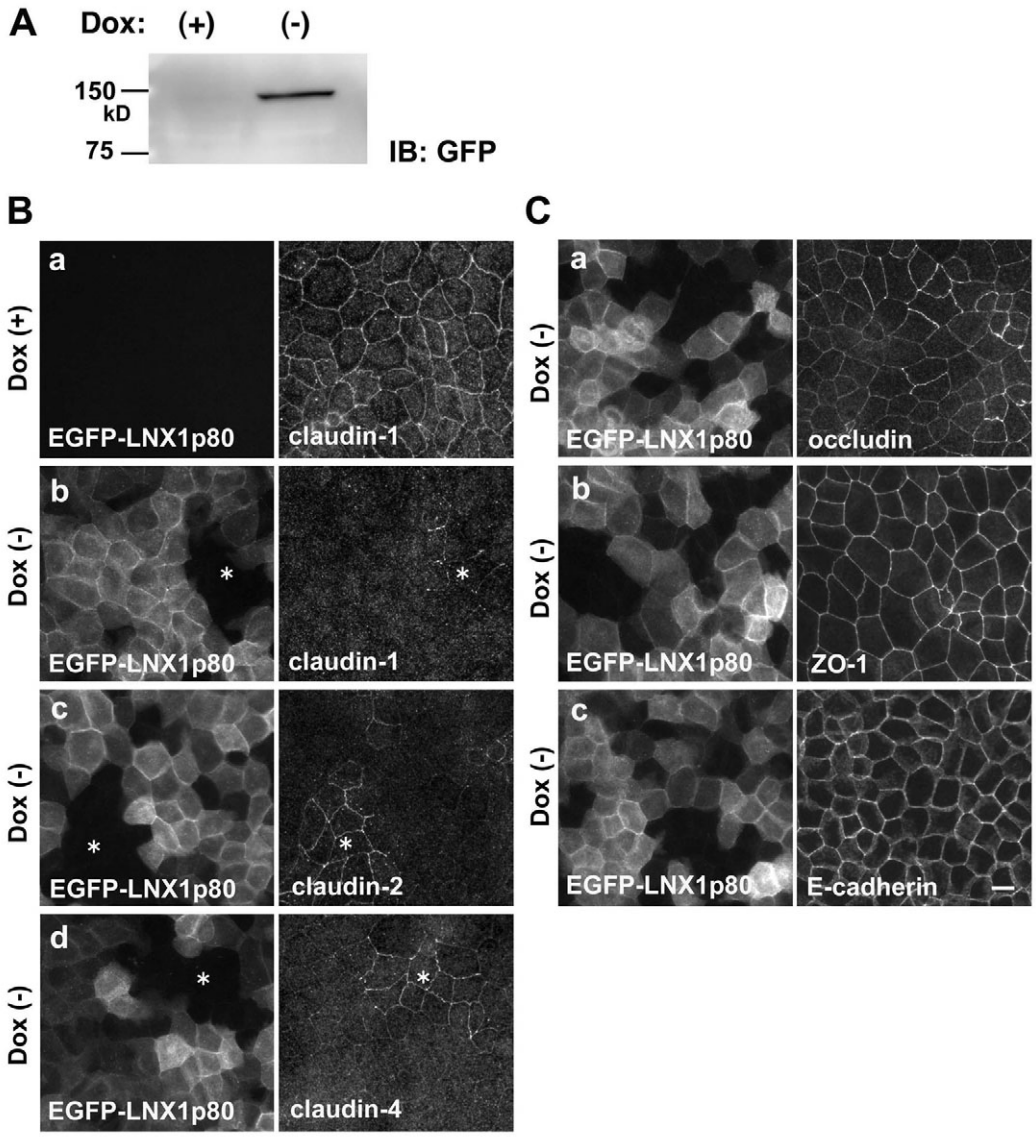


**Fig. 3.** Downregulation of claudins from TJs by inducible expression of LNX1p80 in MDCK cells. (A) Confirmation of the induced expression of EGFP-tagged canine LNX1p80. An MDCK clone that expressed EGFP-tagged canine LNX1p80 (EGFP-LNXp80) under the control of the Tet-Off inducible system (Tet-EGFP-LNX1p80 MDCK cells) was cultured in the presence (+) or absence (–) of doxycycline. Lysates from these cells were separated by SDS-PAGE, followed by immunoblotting with anti-GFP mAb (IB: GFP). (B) Localization of EGFP-LNX1p80 and claudin-1, claudin-2 and claudin-4 in Tet-EGFP-LNX1p80 MDCK cells. Cells were cultured in the presence [Dox (+)] or absence [Dox (–)] of doxycycline and immunofluorescently labeled with pAbs against claudin-1, claudin-2 and claudin-4 (right column). The expression of EGFP-LNX1p80 in the same field was detected by its fluorescent signal (left column). In the presence of doxycycline, there was no expression of EGFP-LNX1p80 and claudin-1 was localized at TJs in all cells (a). By contrast, the junctional concentration of claudin-1 was markedly reduced in EGFP-LNX1p80-induced cells in the absence of doxycycline (b). Even under the induced conditions, EGFP-LNX1p80 was not detected in some cells where claudin-1 was clearly localized at TJs (asterisk in c and d). The junctional concentration of claudin-2 (c) and claudin-4 (d) was also markedly reduced in these cells in EGFP-LNX1p80-induced conditions, except for uninduced cells (asterisks). (C) Localization of occludin, ZO-1, and E-cadherin in Tet-EGFP-LNX1p80 MDCK cells. Occludin was slightly downregulated in induced cells (a). By contrast, no significant change was observed in the localization of ZO-1 (b) and E-cadherin (c). Scale bar: 10 μm.

was transfected instead of Flag-LNX1p80, ubiquitylation occurred only at background levels. Furthermore, no significant ubiquitylation was detected when claudin-1 was replaced with its YV-deleted mutant, which cannot bind to LNX1p80 (Fig. 6A). The interaction of Flag-LNX1p80 or Flag-LNX1p80C48A with claudin-1 in these transfectants was detected by co-precipitation experiments (Fig. 6B). To further investigate the manner of ubiquitylation, ubiquitin was replaced with several ubiquitin mutants. When the ubiquitin K0 mutant, in which all of the lysine residues were substituted with arginine, was used instead of normal ubiquitin in the same assay, the ubiquitylated ladder of claudin-1 became undetectable (Fig. 6C). The ubiquitin K48R mutant with arginine substitution of Lys48, which is known to be used in polyubiquitylation for proteasome-mediated protein degradation (Pickart and Fushman, 2004), did not affect ubiquitylation of claudin-1 (Fig. 6C). These results suggest that LNX1p80-mediated ubiquitylation of claudins is via polyubiquitylation of lysine residue(s) in ubiquitin other than Lys48.

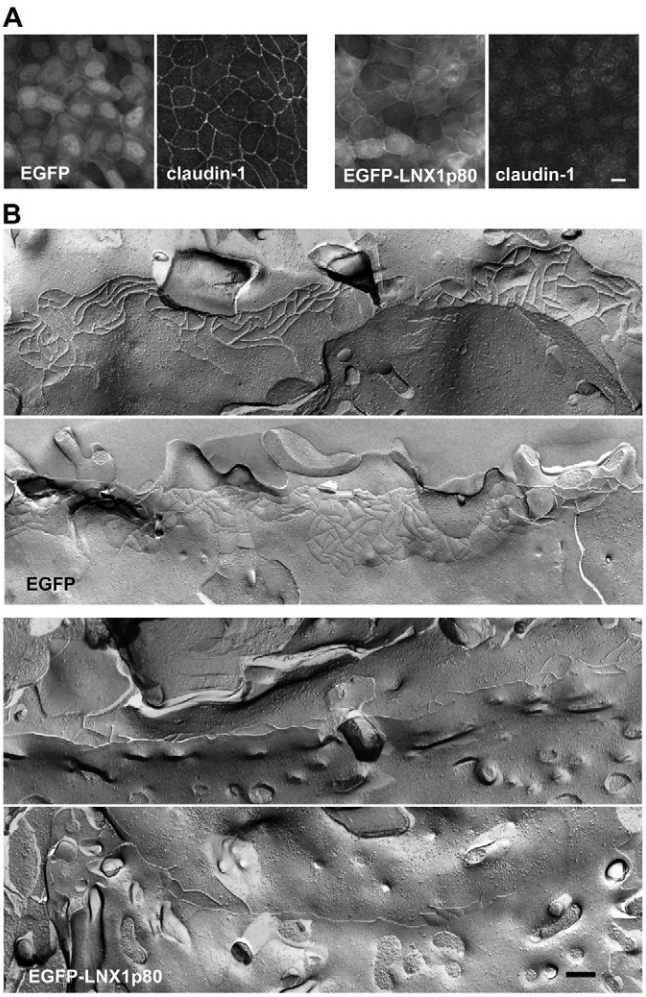


**Fig. 4.** Freeze-fracture replica images of TJ strands in LNX1p80-expressing MDCK cells. (A) Confirmation of downregulation of claudin-1 from TJs in EGFP-LNX1p80-expressing MDCK cells obtained by retrovirus-mediated gene transfer followed by FACS. The signals of EGFP and immunolabeled claudin-1 in EGFP-expressing cells (left) and EGFP-LNX1p80-expressing cells (right) were fluorescently detected. Scale bar: 10 µm. (B) Freeze-fracture replica images of TJ strands. The cells were plated on 24-mm filters, cultured for 3 days, fixed with glutaraldehyde, and then processed for freeze-fracture replica electron microscopy. The number of TJ strands in EGFP-LNX1p80-expressing cells (bottom panels) was obviously lower than that in EGFP-expressing cells (top panels). Scale bar: 200 nm.

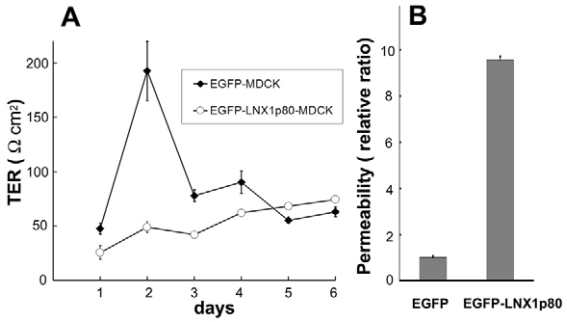


**Fig. 5.** Barrier function of TJs in LNX1p80-expressing MDCK cells. (A) TER measurements. TER in EGFP-expressing MDCK cells transiently reached a maximum at day 2, and then settled to a lower value. This rapid raise of TER around day 2 was never observed in EGFP-LNX1p80-expressing MDCK cells ($n$=6). (B) FITC-dextran flux measurements. Paracellular flux of 4 kDa dextran was significantly increased in EGFP-LNX1p80-expressing MDCK cells compared with control cells (mean ± s.e.m.; $n$=5).

## LNX1p80 is involved in endocytosis and degradation of claudins

The fact that Lys48 of ubiquitin is not primarily used for polyubiquitylation of claudin-1 suggests that the ubiquitylation of claudins is not involved in proteasome-dependent protein degradation, but is involved in several other cell biological processes including endocytosis and intracellular trafficking. We have previously shown that claudins are selectively internalized from TJs by endocytosis and then colocalized with a late endosome marker in intracellular vesicles in cultured epithelial cells (Matsuda et al., 2004). To investigate the involvement of lysosomes in the turnover of claudins, we cultured MDCK cells in the medium containing the lysosome inhibitor chloroquine, and found that the amount of claudin-1 was significantly increased by this treatment (Fig. 7A). However, the proteasome inhibitor MG132 did not increase the amount of claudin-1. These results suggest that claudins are constitutively degraded in lysosomes. Furthermore, chloroquine treatment enhanced the detection of claudin-1 ubiquitylation in EGFP-LNX1p80-expressing but not in EGFP-LNX1p80C48A-expressing MDCK cells (Fig. 7B), confirming that claudin-1 is indeed ubiquitylated by LNX1p80 in MDCK cells in a RING-domain-dependent manner. We then examined the involvement of endocytosis in the LNX1p80-mediated downregulation of claudins from TJs. First, we performed immunofluorescent staining of EGFP-LNX1p80-expressing Tet-Off MDCK cells using anti-claudin-2 mouse monoclonal antibody and rabbit polyclonal antibodies to compartment-specific markers. We found that EGFP-LNX1p80 was partially colocalized with vesicular structures containing claudin-2 (Fig. 8). Furthermore, EGFP-LNX1p80/claudin-2 signals often overlapped with the late endosome marker Rab7 or the lysosome enzyme cathepsin D, suggesting that LNX1p80 is involved in endocytosis of claudins and their transport to lysosomes.

We also examined whether the LNX1p80-induced downregulation of claudins from TJs involves protein degradation. To analyze this, MDCK cells stably expressing EGFP or EGFP-LNX1p80 (described in Fig. 4) were homogenized in a buffer containing 1% NP-40. Western blot analyses showed that the total amount of claudin-1 in the whole lysate of EGFP-LNX1p80-expressing cells was slightly smaller than that of GFP-expressing cells (Fig. 9A,B). For further analyses, the cell lysates were divided into the supernatant and the pellet fractions by centrifugation; these fractions were regarded as the NP-40-soluble and NP-40-insoluble fraction, respectively. In these fractions, we found that NP-40-insoluble claudin-1 in EGFP-LNX1p80-expressing cells was remarkably reduced compared with that in EGFP-expressing cells. The same results were obtained for claudin-2 and claudin-4 (data not shown). By contrast, we found that expression of a RING-domain mutant EGFP-LNX1p80C48A in MDCK cells by the Tet-Off system never resulted in a decease in the total amount of claudin-1 (Fig. 9B). In these cells, claudin-1 accumulation was clearly observed at cell-cell contacts, and often extended to the lateral membrane domain, probably because of a dominant-negative effect (Fig. 9C). The effects of chloroquine and MG132 on the total amount

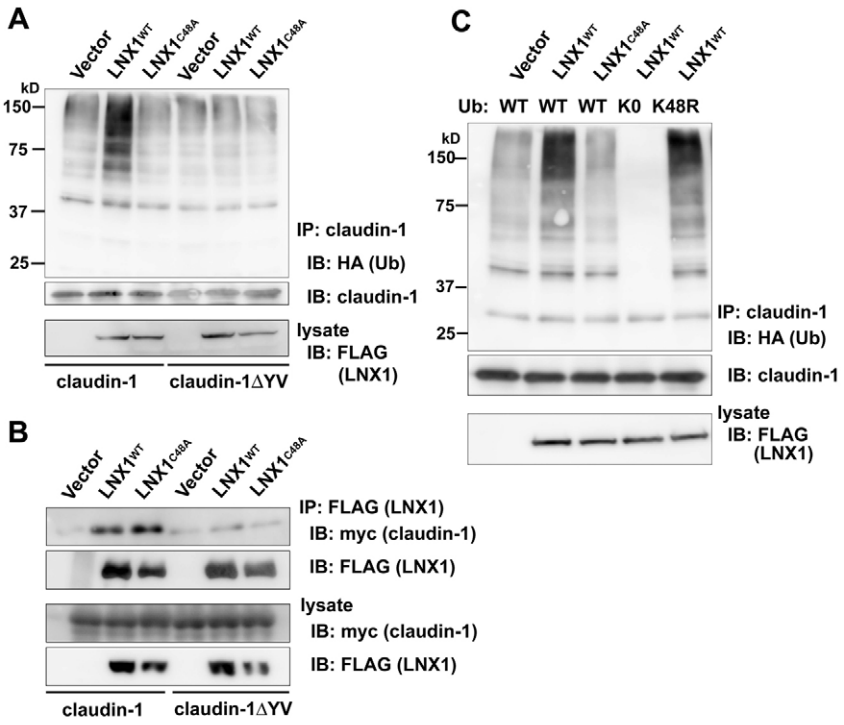


**Fig. 6.** LNX1p80-mediated polyubiquitylation of claudin-1 in HEK293 cells. (A) The expression constructs for Flag-tagged canine LNX1p80, HA-tagged ubiquitin and Myc-tagged claudin-1 were transiently cotransfected into HEK293 cells. Claudin-1 was then immunoprecipitated with anti-claudin-1 pAb, followed by immunoblotting with anti-HA mAb. The combination of Flag-tagged LNX1p80, claudin-1 and HA-ubiquitin exhibited dense ubiquitylation as a smear ($LNX1^{WT}$, lane 2) compared with the lysate without Flag-tagged LNX1p80 (Vector, lane 1) or that with its C48A mutant ($LNX1^{C48A}$, lane 3). When claudin-1 was replaced with the C-terminal YV-deleted mutant (claudin-1ΔYV), only a background level of ubiquitylation was detected. (B) HEK293 cells were transfected as described in A. Flag-tagged LNX1p80 was immunoprecipitated with anti-Flag mAb, followed by immunoblotting with anti-Myc mAb. Myc-tagged claudin-1 was co-precipitated with Flag-tagged LNX1p80 ($LNX1^{WT}$) and LNX1p80C48A ($LNX1^{C48A}$), whereas claudin-1ΔYV was not. (C) Effects of ubiquitin mutants on LNX1p80-mediated ubiquitylation of claudin-1. Lanes 1-3 show a reproduction of lanes 1-3 in A. The K0 mutant of ubiquitin completely abolished the ubiquitylation of claudin-1 by LNX1p80 (lane 4), whereas the K48R mutant never affected it (lane 5).

of claudin-1 in EGFP-LNX1p80- or EGFP-LNX1p80C48A-expressing Tet-Off MDCK cells were similar to those in normal MDCK cells shown in Fig. 7A (data not shown). These observations suggest that the downregulation of claudins by EGFP-LNX1p80 occurs via endocytosis and lysosomal degradation, and that the ubiquitylation activity of LNX1p80 is required for this process.

## Discussion

When epithelial cells move against adjacent cells, intercellular junctions are remodeled. This process must include destruction and generation of each cell junction. In the case of TJs, these two phenomena need to be well coordinated to maintain epithelial barrier function. However, the molecular mechanism behind this regulation of TJ remodeling remains elusive. In the present study, we identified the E3 ubiquitin ligase LNX1p80 as a claudin-binding protein. Our experimental results suggest that LNX1p80 is involved in the dynamic remodeling of TJs via ubiquitylation of claudins, followed by their endocytosis and lysosomal degradation. The ubiquitylation is energy-dependent and is a strictly regulated process with substrate specificity. This feature of ubiquitylation might have a crucial role in the remodeling of TJs, which is likely to be tightly regulated.

LNX1 was originally identified as a binding partner of the phosphotyrosine-binding domain of mammalian Numb in yeast two-hybrid screening (Dho et al., 1998). Among two isoforms of LNX1, LNX1p80 has a RING-finger domain at the N-terminus and is involved in ubiquitin-dependent degradation of Numb (Nie et al., 2002). One or two PDZ domains of LNX1 isoforms have been reported to interact with several molecules, including CAR, JAM4, Src and cytomatrix at the active-zone-associated structural protein (CAST), whose C-termini have PDZ-domain-binding motifs (Sollerbrant et al., 2003; Kansaku et al., 2006; Weiss et al., 2007; Higa et al., 2007). Similarly to these proteins, the C-termini of claudins appear to bind to PDZ domains of LNX1. C-termini of claudins also bind to the PDZ1 domain of ZO-1, ZO-2 and ZO-3, which are TJ-associated plaque proteins (Itoh et al., 1999), suggesting that LNX1 competes with these ZO proteins in claudin binding. ZO-1 and ZO-2 are required for the formation of claudin-based TJs in epithelial cells (Umeda et al., 2006), whereas LNX1p80 seems to work as a negative regulator for TJ formation, as shown in the present study. Therefore, it is of interest how the binding of claudins to LNX1p80 or ZO-1, ZO-2 and ZO-3 is balanced during the remodeling of TJs. The localization of exogenous EGFP-LNX1p80 at TJ regions in MDCK transfectants might be inconsistent with the fact that TJs are remarkably reduced in these cells. There are two possibilities to explain this contradiction. First, EGFP-LNX1p80 might bind to claudins at the remaining TJ strands. Second, EGFP-LNX1p80 might be recruited to TJ regions by binding to the cytoplasmic domain of CAR, which is known to be a TJ-associated membrane protein. Indeed, immunofluorescence staining showed that CAR was localized at TJ regions and the lateral membrane domain, even in EGFP-LNX1p80-expressing MDCK cells (data not shown).

One of the novel findings in this study is that claudins are ubiquitylated by LNX1p80. LNX1p80 has a RING-finger domain, which is assumed to contribute to ubiquitylation by serving as a scaffold that holds both the active site of the ubiquitin-conjugating enzyme E2 and the substrate's acceptor lysine residue (Joazeiro and Weissman, 2000). Consistent with this idea, we found that the C48A mutation in the RING-finger domain of EGFP-LNX1p80 abolished not only the ubiquitylation activity on claudins but also the downregulation of claudins from TJs. Furthermore, the C-terminal-deleted claudin-1, which lacks LNX1p80-binding activity, cannot be ubiquitylated, suggesting that the PDZ domains of LNX1p80 are required as the substrate-binding site for ubiquitylation of claudins. Overexpression of EGFP-LNX1p80 with claudin-1 and ubiquitin in HEK293 cells resulted in a ubiquitylated ladder of claudin-1 as shown by western blotting. Based on the analyses using ubiquitin mutants, this ubiquitylation ladder can be interpreted as

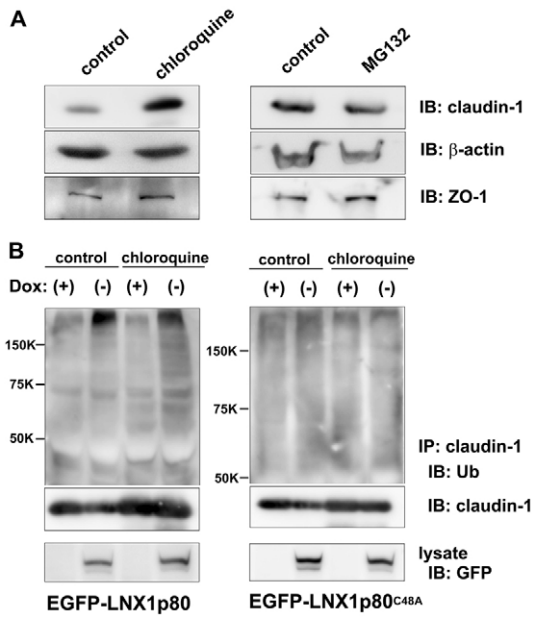


**Fig. 7.** Lysosomal degradation and LNX1p80-promoted ubiquitylation of claudin-1 in MDCK cells. (A) The effect of the lysosome inhibitor chloroquine and the proteasome inhibitor MG132 on the amount of claudin-1. MDCK cells were treated with 100 mM chloroquine or 10 mM MG132 for 18 hours and processed for SDS-PAGE followed by immunoblotting with anti-claudin-1 pAb, anti-β-actin mAb and anti-ZO-1 mAb. Chloroquine treatment increased the amount of claudin-1, indicating that claudin-1 is degraded in the lysosome. MG132 treatment did not affect the amount of claudin-1. With both treatments, the amounts of β-actin and ZO-1 did not significantly change. (B) Ubiquitylation of claudin-1 by LNX1p80 in MDCK cells. Tet-EGFP-LNX1p80 MDCK cells and EGFP-tagged canine LNX1p80C48A-expressing MDCK cells under the control of the Tet-Off system (Tet-EGFP-LNX1p80C48A MDCK cells) were cultured with or without doxycycline (Dox+ and Dox–). Claudin-1 was immunoprecipitated, followed by immunoblotting with anti-ubiquitin mAb. Ubiquitylation of claudin-1 was increased in Tet-EGFP-LNX1p80 MDCK cells treated with 100 mM of chloroquine for 18 hours. In Tet-EGFP-LNX1p80C48A MDCK cells, only the background level of ubiquitylation was detected.

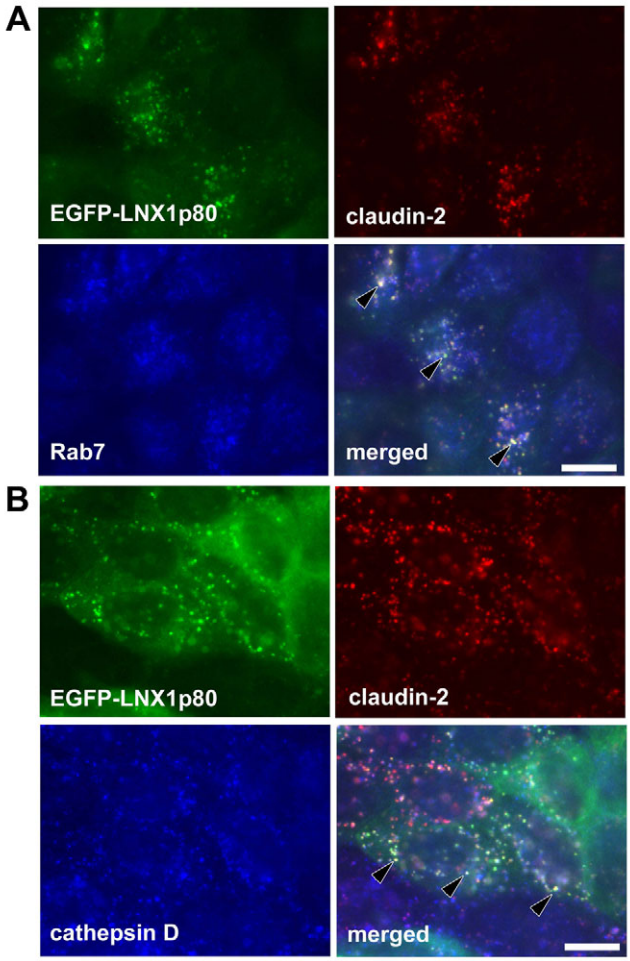


**Fig. 8.** Colocalization of claudin-2 with LNX1p80 and an endocytic marker in LNX1p80-expressing MDCK cells. Tet-EGFP-LNX1p80 MDCK cells (described in Fig. 3) were immunofluorescently stained with anti-claudin-2 mAb and anti-Rab7 pAb (A) or anti-cathepsin D pAb (B) under the induction of EGFP-LNX1p80 expression. Claudin-2, EGFP-LNX1p80, and Rab7 or cathepsin D were often colocalized in intracellular vesicular structures (arrowheads). Since different planes were analyzed using a ×100 objective lens with a large numerical aperture, the concentration of EGFP-LNX1p80 at cell-cell contacts was not visible in these images. Scale bars: 10 μm.

polyubiquitylation of lysine residue(s), except for Lys48, whose ubiquitylation is a hallmark of proteasome-mediated protein degradation (Pickart and Fushman, 2004). In addition to monoubiquitylation, polyubiquitylation of some lysine residues of ubiquitin is known to contribute to various cellular functions other than proteasome-mediated degradation, including endocytosis and lysosomal degradation (Mukhopadhyay and Riezman, 2007). There are several lysine residues that are possible ubiquitylation sites, in cytoplasmic domains of claudin-1, claudin-2 and claudin-4 at the C-terminal cytoplasmic domains, as well as intracellular turns (Furuse et al., 1998a). Determination of ubiquitylation sites within claudins and ubiquitin, as well as in vitro reconstitution of ubiquitylation, are required for further understanding of the molecular mechanism of LNX1p80-mediated ubiquitylation of claudins.

Downregulation of claudins from TJs in EGFP-LNX1p80-expressing MDCK cells can be interpreted by two possible mechanisms: the internalization of claudins from TJs is accelerated or the incorporation of claudins into TJs is inhibited. The former idea is more likely because ubiquitylation is often used as a signal for triggering endocytosis, and we found that EGFP-LNX1p80, as well as claudins, were at least partially colocalized with Rab7 and cathepsin D, which are markers for endocytic processes. We have previously shown that claudins are frequently endocytosed from TJs in cultured epithelial cells by live observation (Matsuda et al., 2004). The manner of this endocytosis is unusual; claudins at TJs are internalized into one of the adjoining cells as vesicles, maintaining an attachment between apposed membranes. These vesicles do not contain EEA1, a marker of early endosomes, but are partially colocalized with Rab7, a late endosome marker. Interestingly, this endocytosis of claudins occurs without simultaneous internalization of occludin and ZO-1, indicating that claudins are segregated within TJs and then engulfed into the cell (Matsuda et al., 2004). LNX1p80 seems to be involved in this process by specific ubiquitylation of claudins followed by endocytosis. In our study, compared with remarkable downregulation of claudins from TJs in EGFP-LNX1p80-expressing MDCK cells, the reduction of occludin from TJs was moderate,

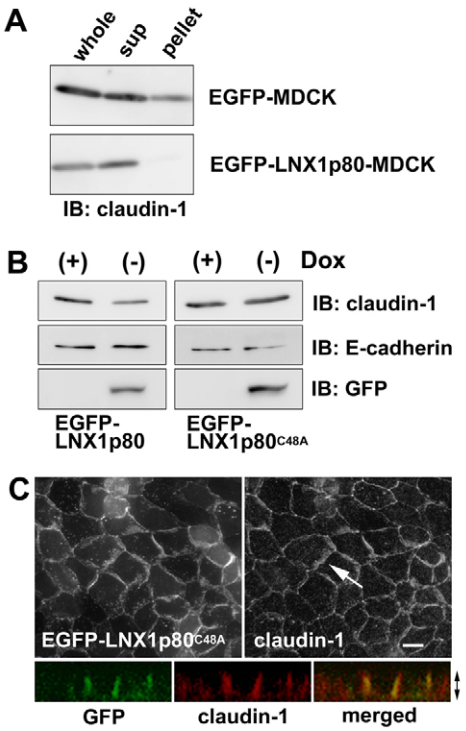


**Fig. 9.** Effects of LNX1p80 expression on the amount of endogenous claudin-1 protein in MDCK cells. (A) Reduction in the amount of claudin-1 by LNX1p80 expression in MDCK cells. Western blot of the whole lysate (whole), 1% NP-40-soluble (sup) and insoluble (pellet) fraction of MDCK cells constitutively expressing EGFP or EGFP-LNX1p80 with anti-claudin-1 pAb. The amount of NP-40-insoluble claudin-1 (pellet) was remarkably reduced in cells expressing EGFP-LNX1p80 compared with that in EGFP-expressing MDCK cells. (B) The effect of RING-domain mutant of LNX1p80 on claudin-1. Tet-EGFP-LNX1p80 MDCK cells and Tet-EGFP-LNX1p80C48A MDCK cells were cultured with (+) or without (–) doxycycline. The amounts of claudin-1, E-cadherin, EGFP-LNX1p80 and EGFP-LNX1p80C48A in total cell lysates were analyzed by immunoblotting with anti-claudin-1 pAb, anti-E-cadherin mAb and anti-GFP mAb. The total claudin-1 protein level was decreased in EGFP-LNX1p80-expressing cells, but not in EGFP-LNX1p80C48A-expressing cells. The amount of E-cadherin did not change in this experiment. (C) Immunofluorescence localization of claudin-1 in MDCK cells expressing EGFP-LNX1p80C48A. Tet-EGFP-LNX1p80C48A MDCK cells cultured without doxycycline were immunostained with anti-claudin-1 pAb. Vertical sections were obtained by confocal microscopy (lower panel). The concentration of claudin-1 was not limited to TJ regions but also extended to the lateral membrane (arrow). EGFP-LNX1p80C48A was colocalized with claudin-1. Scale bar: 10 μm.

which might be a secondary effect of claudin downregulation. The localization of ZO-1 was not affected in these cells. These observations indicate that LNX1p80 has a crucial role in the selective internalization of claudins from TJs. When considering the general interpretation that adhesion molecules incorporated into junctional structures are detergent-insoluble (Hirano et al., 1987; Sakakibara et al., 1997), the decrease in the amount of NP-40-insoluble claudins in EGFP-LNX1p80-expressing MDCK cells in our study corresponds well with the downregulation of claudins from TJs. However, the amount of NP-40-soluble claudins in these cells did not change markedly. Taken together, these observations imply that TJ-incorporated claudins are selectively recognized by LNX1p80 for ubiquitylation and internalization followed by lysosome targeting by unknown mechanisms.

Although the overexpression of LNX1p80 resulted in a striking downregulation of TJs in MDCK cells, its physiological function in TJs remains unclear. It would be interesting to investigate the expression and localization of LNX1p80 in the cellular process in which the turnover of TJs was accelerated because of cell division and dynamic rearrangement of epithelial cells during development. It is also tempting to speculate that LNX1p80 activity regulates the morphology of TJs. In this study, overexpression of LNX1p80 resulted in a remarkable decrease in the number of TJ strands, whereas the expression of LNX1p80C48A, which is a ubiquitylation-deficient mutant (Nie et al., 2002), resulted in the extension of the TJ area in the basal direction of the lateral membrane. This finding suggests that LNX1p80 negatively regulates the number of TJ strands. The number and complexity of TJ strands visualized by freeze-fracture replica electron microscopy vary among cell types (Claude and Goodenough, 1973). In the kidney, for example, TJs in the proximal tubule consist of only one or two TJ strands, whereas those in the collecting duct have many more. Although such variation appears to depend on the physiological requirement of each cell type, it remains unclear how the mass of TJs is regulated. In addition to the control of TJ formation by the scaffold proteins ZO-1 and ZO-2, LNX1p80 might be involved in the mass control of TJs by regulating the turnover of claudins. Finally, it is of interest whether Numb has a role in LNX1-induced reduction of TJs. Because Numb has been recently identified as an endocytic protein (Santolini et al., 2000), it might be involved in endocytic internalization of claudins via complex formation with LNX1. To investigate these issues further, the expression of LNX1p80 protein in cultured cells and tissues should be described with its specific antibodies. Furthermore, experiments on the suppression of LNX1p80 expression by RNA interference or the expression of a dominant-negative form of LNX1p80 in cultured epithelial cells are also needed to clarify the physiological function of LNX1p80. These types of investigations will hopefully lead to a better understanding of the complex and will probably reveal a sophisticated mechanism behind the dynamic remodeling of TJs.

## Materials and Methods

### Antibodies and cells

Rabbit anti-claudin-2 polyclonal antibody (pAb), guinea pig anti-claudin-1 pAb, rabbit anti-claudin-4 pAb were raised and characterized as described previously (Furuse et al., 1999; Morita et al., 1999). Mouse anti-ZO-1 monoclonal antibody (mAb) (T8-754) and rat anti-occludin mAb (MOC37) were raised and characterized as described previously (Itoh et al., 1991; Saitou et al., 1997). Rat anti-E-cadherin mAb (ECCD2), rabbit anti-Rab7 pAb, rabbit anti-cathepsin D pAb and rabbit anti-CAR pAb were kindly provided by Masatoshi Takeichi (Riken, Kobe, Japan), Ge-Hong Sun-Wada (Doshisha Women's College of Liberal Arts, Kyoto, Japan), Kazumi Ishidoh (Tokushima Bunri University, Tokushima, Japan), and Jeffrey M. Bergelson (University of Pennsylvania, Philadelphia, PA), respectively. Mouse anti-GFP mAb (Roche Diagnostic K.K.), rat anti-HA mAb (3F10; Roche), mouse anti-HA mAb (12CA5; Roche), mouse anti-Flag mAb (M2; Sigma), rabbit anti-DDDDK-tag pAb (MBL), rabbit anti-claudin-1 pAb and mouse anti-claudin-2 mAb (Zymed Labs) and mouse anti-ubiquitin mAb (P4G7; Covance) were obtained by commercial resources. Epithelial cell line, MDCK II, was generously donated by Masayuki Murata (The University of Tokyo, Tokyo, Japan). A potent retrovirus packaging cell line, PLAT-E, was a kind gift from Toshio Kitamura (The University of Tokyo, Tokyo, Japan). MDCK II VR20 expressing the ecotropic mouse retrovirus receptors was described and characterized previously (Matsuda et al., 2008). MDCK Tet-Off cell line was purchased from Clontech. All cells were cultured in Dulbecco's modified Eagle's medium (DMEM) supplemented with 10% fetal calf serum.

### Yeast two-hybrid screening

To construct the bait vector, the cDNA fragment encoding the C-terminal region (a.a. 188-211) of mouse claudin-1 was amplified by PCR and subcloned into pBTM116 containing the LexA DNA-binding domain and a tryptophan marker. This vector was introduced into yeast cells (strain L40) followed by selection on medium lacking

tryptophan. Then, the yeast cells harboring bait plasmids were transformed with a mouse brain cDNA library (Clontech) that had been generated with pACT2 containing the GAL4 transactivating domain and a leucine marker. About $1\times10^7$ yeast transformants were plated on synthetic complete medium lacking histidine, leucine, and tryptophan, and 34 colonies were picked up after incubation for 48-96 hours. Of these, 15 were selected as positive clones by a β-galactosidase assay. Prey plasmids were recovered from these positive clones, and the sequences of their inserts were determined.

### GST pull-down assay

The GST-fusion proteins with the C-terminal cytoplasmic domain of claudin-1, RKTTSYPTPRPYPKPTPSSGKDYV (GST-cld1C), and its mutant lacking C-terminal tyrosine and valine (GST-cld1CΔYV) generated in *Escherichia coli* were bound to glutathione-Sepharose beads and incubated with the lysate of HEK293 cells expressing HA-tagged mouse LNX1p80. After washing, bound proteins were eluted together with these GST-fusion proteins and separated by SDS-PAGE, followed by immunoblotting with anti-HA mAb.

### SDS-PAGE and immunoblotting

Samples were separated by one-dimensional SDS-PAGE. For immunoblotting, proteins were electrophoretically transferred from gels onto polyvinylidene difluoride (PVDF) membranes (Immobilon-P, Millipore), which were then incubated with primary antibodies. Bound antibodies were detected with horseradish-peroxidase-conjugated secondary antibodies (GE Healthcare). ECL plus reagents (GE Healthcare) were used as substrates for detection of peroxidase.

### Expression constructs and transfection

Plasmid constructs for the expression of HA-tagged ubiquitin and its mutants K0 and K48R (pcDNA3.1-HA-Ub, pcDNA3.1-HA-$Ub^{K0}$, pcDNA3.1-HA-$Ub^{K48R}$) were kindly provided by Keiji Tanaka and Shigeo Murata (The Tokyo Metropolitan Institute of Medical Science, Tokyo, Japan). pUHD10-3 and pMX were generously donated by Shunichi Takeda (Kyoto University, Kyoto, Japan) and Toshio Kitamura (The University of Tokyo, Tokyo, Japan), respectively. To obtain the full-length cDNA of mouse LNX1p80, its N-terminal half was amplified from mouse brain total RNA by RT-PCR, and combined with its C-terminal half obtained by yeast two-hybrid screening at the *Bam*HI site. The full-length cDNA of canine LNX1p80 was obtained from MDCK II total RNA by RT-PCR amplification according to database information (GenBank accession number XP_849707). To obtain LNX1p80 C48A mutant, the nucleotide sequence 'TGC' encoding Cys48 of canine LNXp80 was replaced with 'GCC' for alanine substitution via site-directed in vitro mutagenesis. These cDNAs were tagged with EGFP, Flag or HA and subcloned into pCAGGSneodelEcoRI (Niwa et al., 1991) or pUHD10-3 for constitutive or inducible expression, respectively. To induce protein expression in Tet-Off MDCK cells, doxycycline was omitted from the culture medium, whereas 20 ng/ml doxycycline was included to suppress expression. The cultured epithelial cells were transfected with the expression vectors in serum-free DMEM with 50 μM $CaCl_2$ using LipofectAmine Plus (Invitrogen). The cells transfected with pCAGGS-derived expression vectors were cultured in a selection medium containing 400 μg/ml G418. pUHD10-3-derived plasmids were cotransfected with pSV2 hph into MDCK Tet-Off cell line, which were then cultured in a selection medium containing 150 μg/ml of hygromycin B. After selection for 2 weeks, resistant clones were separated and screened by fluorescence microscopy. MDCK cells expressing EGFP-tagged canine LNX1p80 (EGFP-LNX1p80) were also established via retrovirus-mediated gene transfer. EGFP-LNX1p80 cDNA was subcloned into the mouse retrovirus vector pMX and the plasmid was converted to retroviruses in Plat-E packaging cells. MDCKIIVR20 cells were then infected with this retrovirus as described previously (Matsuda et al., 2008).

### Immunofluorescence microscopy

Cells cultured on coverslips were fixed with 1% formaldehyde in PBS for 10 minutes, followed with 0.2% Triton X-100 in PBS for 10 minutes. After washing with PBS, the fixed cells were blocked with 1% bovine serum albumin in PBS. Samples were then incubated with primary antibodies for 30 minutes at room temperature, followed by incubation with secondary antibodies for 30 minutes. After rinsing with PBS, cells were embedded in Fluorsave (Calbiochem). Images were obtained using an IX70 or IX71 microscope (Olympus) equipped with a UPlanApo ×40 (NA 0.85) or UPlanApo ×100 oil (NA 1.35) objective, and a cooled charge-coupled device camera (ORCA-AG, Hamamatsu). Vertical section images were obtained using a DMI4000B microscope (Leica) equipped with a confocal microscope system TCS SPE (Leica).

### Freeze-fracture electron microscopy

MDCK cells expressing EGFP-LNX1p80 or EGFP obtained by using retrovirus vectors were trypsinized, and GFP-positive cells were collected by fluorescence-activating cell sorting (FACS). Each cell population was then propagated. For electron microscopic analyses, one hundredth of confluent cells on 10 cm cultured dishes were plated on a 24 mm Transwell filter (Corning) for 3 days. Cells were fixed with 2% glutaraldehyde in 0.1 M phosphate buffer (PB), immersed overnight in 30% glycerol in 0.1M PB, and then frozen in liquid nitrogen. Frozen samples were fractured at –100°C and platinum-shadowed unidirectionally at an angle of 45° in Balzers Freeze Etching System (BAF060; BAL-TEC). Samples were picked up on formovar-filmed grids and examined with a Hitachi H-7500 electron microscope at an acceleration voltage of 100 kV.

### Measurement of TER and paracellar tracer flux

Aliquots of $1\times10^5$ cells were plated on 12 mm Transwell filters (Corning), and the culture medium was changed each day. TER was measured directly in culture medium using a Millicell-ERS epithelial voltohmmeter (Millipore). The TER values were calculated by subtracting the background TER of blank filters, followed by multiplying by the surface area of the filter. For the paracellular tracer flux assay, 4 kDa FITC-dextran was added to the medium in the apical compartment of cells at day 6 at a concentration of 1 mg/ml. After incubation for 2 hours, an aliquot of medium was collected from the basal compartment. The paracellular tracer flux was determined as the amount of FITC-dextran in the basal medium, which was measured with a fluorometer.

### Preparation and fractionation of cell lysates

MDCK cells expressing EGFP-LNX1p80 or EGFP were cultured on 60 mm dishes, washed three times with ice-cold PBS, and then lysed in 500 μl NP-40-IP buffer as described previously (Sakakibara et al., 1997). After scraping into a microcentrifuge tube, cells were gently rotated for 30 minutes at 4°C, followed by centrifugation at 10,000 ***g*** for 30 minutes. The supernatant and the same volume of buffer added to the pellet were regarded as the NP-40-soluble and NP40-insoluble fraction, respectively.

### Immunoprecipitation

The expression constructs for Flag-tagged canine LNX1p80, HA-tagged ubiquitin and N-terminal Myc-tagged claudin-1 were transiently cotransfected into HEK293 cells using LipofectAmine Plus. After 36 hours, cells were lysed in RIPA buffer containing N-ethylmaleimide (NEM) (0.1% SDS, 0.5% sodium deoxycholate, 1% NP-40, 50 mM Tris-HCl, 150 mM NaCl, 10 mM NEM and protease inhibitors). Cell lysates were gently rotated for 30 minutes at 4°C and centrifuged at 15,000 rpm for 10 minutes. Protein-G-Sepharose 4 Fast Flow (GE Healthcare), which had been preincubated with guinea pig anti-claudin-1 pAb or mouse anti-Flag mAb (M2), was added to the supernatant and incubated for 1 hour at 4°C, followed by separation by SDS-PAGE. For detection of claudin-1 ubiquitylation in MDCK cells, claudin-1 was immunoprecipitated with guinea pig anti-claudin-1 pAb from cell lysates prepared as described above, followed by immunoblotting with anti-ubiquitin mAb. Ubiquitylation was detected with or without 100 mM chloroquine treatment for 18 hours.

We thank S. Seino and K. Ishizaki for their assistance with fluorescence-activated cell sorting; K. Tanaka and S. Murata for providing ubiquitin constructs; Y. Fujita and D. Morito for advice on ubiquitylation assay; and all members of our laboratory for helpful discussions. We also thank KAN Research Institute for support with freeze-fracture electron microscopy. This study was supported by a Grant-in-Aid for Cancer Research and the National Project on Targeted Protein Research Program (TPRP) from the Ministry of Education, Culture, Sports, Science and Technology of Japan, and grants from Takeda Science Foundation, Uehara Memorial Foundation and The Cell Science Research Foundation to M.F.

## References

**Angelow, S., Ahlstrom, R. and Yu, A. S.** (2008). Biology of claudins. *Am. J. Physiol. Renal Physiol*. 295, F867-F876.

**Baker, J. and Garrod, D.** (1993). Epithelial cells retain junctions during mitosis. *J. Cell Sci.* **104**, 415-425.

**Chiba, H., Osanai, M., Murata, M., Kojima, T. and Sawada, N.** (2008). Transmembrane proteins of tight junctions. *Biochim. Biophys. Acta* **1778**, 588-600.

**Claude, P. and Goodenough, D. A.** (1973). Fracture faces of zonulae occludentes from "tight" and "leaky" epithelia. *J. Cell Biol.* **58**, 390-400.

**d'Azzo, A., Bongiovanni, A. and Nastasi, T.** (2005). E3 ubiquitin ligases as regulators of membrane protein trafficking and degradation. *Traffic* **6**, 429-441.

**Dho, S. E., Jacob, S., Wolting, C. D., French, M. B., Rohrschneider, L. R. and McGlade, C. J.** (1998). The mammalian numb phosphotyrosine-binding domain. Characterization of binding specificity and identification of a novel PDZ domain-containing numb binding protein, LNX. *J. Biol. Chem.* **273**, 9179-9187.

**Fujita, Y., Krause, G., Scheffner, M., Zechner, D., Leddy, H. E., Behrens, J., Sommer, T. and Birchmeier, W.** (2002). Hakai, a c-Cbl-like protein, ubiquitinates and induces endocytosis of the E-cadherin complex. *Nat. Cell Biol.* **4**, 222-231.

**Furuse, M. and Tsukita, S.** (2006). Claudins in occluding junctions of humans and flies. *Trends Cell Biol.* **16**, 181-188.

**Furuse, M., Fujita, K., Hiiragi, T., Fujimoto, K. and Tsukita, S.** (1998a). Claudin-1 and -2: novel integral membrane proteins localizing at tight junctions with no sequence similarity to occludin. *J. Cell Biol.* **141**, 1539-1550.

**Furuse, M., Sasaki, H., Fujimoto, K. and Tsukita, S.** (1998b). A single gene product, claudin-1 or -2, reconstitutes tight junction strands and recruits occludin in fibroblasts. *J. Cell Biol.* **143**, 391-401.

**Furuse, M., Sasaki, H. and Tsukita, S.** (1999). Manner of interaction of heterogeneous claudin species within and between tight junction strands. *J. Cell Biol.* **147**, 891-903.

**Gumbiner, B. M.** (1996). Cell adhesion: the molecular basis of tissue architecture and morphogenesis. *Cell* **84**, 345-357.

**Hershko, A. and Ciechanover, A.** (1998). The ubiquitin system. *Annu. Rev. Biochem.* **67**, 425-479.

**Hicke, L. and Dunn, R.** (2003). Regulation of membrane protein transport by ubiquitin and ubiquitin-binding proteins. *Annu. Rev. Cell Dev. Biol.* **19**, 141-172.

**Higa, S., Tokoro, T., Inoue, E., Kitajima, I. and Ohtsuka, T.** (2007). The active zone protein CAST directly associates with Ligand-of-Numb protein X. *Biochem. Biophys. Res. Commun.* **354**, 686-692.

**Hirano, S., Nose, A., Hatta, K., Kawakami, A. and Takeichi, M.** (1987). Calcium-dependent cell-cell adhesion molecules (cadherins): subclass specificities and possible involvement of actin bundles. *J. Cell Biol.* **105**, 2501-2510.

**Itoh, M., Yonemura, S., Nagafuchi, A., Tsukita, S. and Tsukita, S.** (1991). A 220-kD undercoat-constitutive protein: its specific localization at cadherin-based cell-cell adhesion sites. *J. Cell Biol.* **115**, 1449-1462.

**Itoh, M., Furuse, M., Morita, K., Kubota, K., Saitou, M. and Tsukita, S.** (1999). Direct binding of three tight junction-associated MAGUKs, ZO-1, ZO-2, and ZO-3, with the COOH termini of claudins. *J. Cell Biol.* **147**, 1351-1363.

**Jinguji, Y. and Ishikawa, H.** (1992). Electron microscopic observations on the maintenance of the tight junction during cell division in the epithelium of the mouse small intestine. *Cell Struct. Funct.* **17**, 27-37.

**Joazeiro, C. A. and Weissman, A. M.** (2000). RING finger proteins: mediators of ubiquitin ligase activity. *Cell* **102**, 549-552.

**Kansaku, A., Hirabayashi, S., Mori, H., Fujiwara, N., Kawata, A., Ikeda, M., Rokukawa, C., Kurihara, H. and Hata, Y.** (2006). Ligand-of-Numb protein X is an endocytic scaffold for junctional adhesion molecule 4. *Oncogene* **25**, 5071-5084.

**Matsuda, M., Kubo, A., Furuse, M. and Tsukita, S.** (2004). A peculiar internalization of claudins, tight junction-specific adhesion molecules, during the intercellular movement of epithelial cells. *J. Cell Sci.* **117**, 1247-1257.

**Matsuda, M., Kobayashi, Y., Masuda, S., Adachi, M., Watanabe, T., Yamashita, J. K., Nishi, E., Tsukita, S. and Furuse, M.** (2008). Identification of adherens junction-associated GTPase activating proteins by the fluorescence localization-based expression cloning. *Exp. Cell Res.* **314**, 939-949.

**Morita, K., Furuse, M., Fujimoto, K. and Tsukita, S**. (1999). Claudin multigene family encoding four-transmembrane domain protein components of tight junction strands. *Proc. Natl. Acad. Sci. USA* **96**, 511-516.

**Mukhopadhyay, D. and Riezman, H.** (2007). Proteasome-independent functions of ubiquitin in endocytosis and signaling. *Science* **315**, 201-205.

**Nie, J., McGill, M. A., Dermer, M., Dho, S. E., Wolting, C. D. and McGlade, C. J.** (2002). LNX functions as a RING type E3 ubiquitin ligase that targets the cell fate determinant Numb for ubiquitin-dependent degradation. *EMBO J.* **21**, 93-102.

**Niwa, H., Yamamura, K. and Miyazaki, J.** (1991). Efficient selection for high-expression transfectants with a novel eukaryotic vector. *Gene* **108**, 193-199.

**Pickart, C. M. and Fushman, D.** (2004). Polyubiquitin chains: polymeric protein signals. *Curr. Opin. Chem. Biol.* **8**, 610-616.

**Powell, D. W.** (1981). Barrier function of epithelia. *Am. J. Physiol.* **241**, G275-G288.

**Saitou, M., Ando-Akatsuka, Y., Itoh, M., Furuse, M., Inazawa, J., Fujimoto, K. and Tsukita, S.** (1997). Mammalian occludin in epithelial cells: its expression and subcellular distribution. *Eur. J. Cell Biol.* **73**, 222-231.

**Sakakibara, A., Furuse, M., Saitou, M., Ando-Akatsuka, Y. and Tsukita, S.** (1997). Possible involvement of phosphorylation of occludin in tight junction formation. *J. Cell Biol.* **137**, 1393-1401.

**Santolini, E., Puri, C., Salcini, A. E., Gagliani, M. C., Pelicci, P. G., Tacchetti, C. and Di Fiore, P. P.** (2000). Numb is an endocytic protein. *J. Cell Biol.* **151**, 1345-1352.

**Schock, F. and Perrimon, N.** (2002). Molecular mechanisms of epithelial morphogenesis. *Annu. Rev. Cell Dev. Biol.* **18**, 463-493.

**Sollerbrant, K., Raschperger, E., Mirza, M., Engstrom, U., Philipson, L., Ljungdahl, P. O. and Pettersson, R. F.** (2003). The Coxsackievirus and adenovirus receptor (CAR) forms a complex with the PDZ domain-containing protein ligand-of-numb protein-X (LNX). *J. Biol. Chem.* **278**, 7439-7444.

**Traweger, A., Fang, D., Liu, Y. C., Stelzhammer, W., Krizbai, I. A., Fresser, F., Bauer, H. C. and Bauer, H.** (2002). The tight junction-specific protein occludin is a functional target of the E3 ubiquitin-protein ligase itch. *J. Biol. Chem.* **277**, 10201-10208.

**Umeda, K., Ikenouchi, J., Katahira-Tayama, S., Furuse, K., Sasaki, H., Nakayama, M., Matsui, T., Tsukita, S., Furuse, M. and Tsukita, S.** (2006). ZO-1 and ZO-2 independently determine where claudins are polymerized in tight-junction strand formation. *Cell* **126**, 741-754.

**Van Itallie, C. M. and Anderson, J. M.** (2006). Claudins and epithelial paracellular transport. *Annu. Rev. Physiol.* **68**, 403-429.

**Weiss, A., Baumgartner, M., Radziwill, G., Dennler, J. and Moelling, K.** (2007). c-Src is a PDZ interaction partner and substrate of the E3 ubiquitin ligase Ligand-of-Numb protein X1. *FEBS Lett.* **581**, 5131-5136.